Electronic Properties of Bulk and Single-Layer MoS2 Using ab Initio DFT: Application of Spin-Orbit Coupling (SOC) Parameters

Article *in* East European Journal of Physics · January 2020

DOI: 10.26565/2312-4334-2020-4-09

CITATIONS
2

READS
174

2 authors:

Gyan Michael
University of Electronic Science and Technology of China
14 PUBLICATIONS **51** CITATIONS
SEE PROFILE

Joseph Parbey
University of Electronic Science and Technology of China
20 PUBLICATIONS **200** CITATIONS
SEE PROFILE

East Eur. J. Phys. **4**. 69-74 (2020) DOI:10.26565/2312-4334-2020-4-09

PACS: 71.15.mb

ELECTRONIC PROPERTIES OF BULK AND SINGLE-LAYER MOS_2 USING AB INITIO DFT: APPLICATION OF SPIN-ORBIT COUPLING (SOC) PARAMETERS

Michael Gyan[a,*], Francis E. Botchway[b,c], Joseph Parbey[a,b,c]
[a]*School of Physics, University of Electronic Science and Technology of China, Chengdu 610054, China*
[b]*School of Material Science, University of Electronic Science and Technology of China, Chengdu 610054, China*
[c]*Koforidua, Technical University, Ghana*
**Corresponding Author: mgyan173@gmail.com; phone: +8613228202349*
Received September 2, 2020; accepted November 4, 2020

Two dimensional (2D) materials are currently gaining a lot of interest due to excellent properties that are different from their bulk structures. Single and few-layered of Transition metal dichalcogenides (TMDCs) have a bandgap that ranges between 1-2 eV, which is used for FET devices or any optoelectronic devices. Within TMDCs, a ton of consideration is focused on Molybdenum Disulfide (MoS2) because of its promising band gap-tuning and transition between direct to indirect bandgap properties relies upon its thickness. The density functional theory (DFT) calculations with different functionals and spin-orbit coupling (SOC) parameters were carried out to study the electronic properties of bulk and monolayer MoS_2. The addition of SOC brought about a noteworthy change in the profile of the band energy, explicitly the splitting of the valence band maximum (VBM) into two sub-bands. The indirect bandgap in bulk MoS_2 ranges from 1.17-1.71 eV and that of the monolayer bandgap was 1.6-1.71 eV. The calculated parameters were compared to the obtained experimental and theoretical results. The obtained density of states (DOS) can be used in explaining the nature of bandgap in both the bulk and monolayer MoS_2. These electronic characteristics are important for applications in material devices and energy-saving applications.
KEYWORDS: Electronic properties, Density functional theory, Spin-orbit coupling, Density of states, MoS_2, bandgap

One of the greatest discoveries in science is the successful flaking of graphene into a 2D sheet of carbon in 2004 by Novoselov et al [1]. Graphene exhibits excellent mechanical, electronic, and physical properties. It's unanticipated Zero bandgap limits its applications [2, 3]. The introduction of graphene has resulted in a great interest in other 2D materials such as phosphorene [4], silicone [5], TMDCs [6], and monochalcogenides [7, 8], creating huge attention in Nanoelectronic and optoelectronic devices [9-11]. From the various available 2D materials, 2D TMDCs exhibits superb physical properties like large bandgap which is needed in Photocatalytic water splitting [12,13].

Layered TMDCs materials are the best candidates for 2D materials because their bandgap lies between 1 to 2 eV [14]. Within the TMDCs, MoS_2 is the most sought for due to its industrial application starting from the use in lubricant [15], energy storage [16], photovoltaics [17], and catalyst [18]. Bulk MoS_2 is a semiconductor having an indirect bandgap of 1.23 eV, with its monolayer possessing a direct energy bandgap of 1.8 eV [19]. The electronic structure undergoes an excellent transition upon exfoliation from the bulk [1, 19-23]. Currently, field-effect transistor (FET) based on single-layer MoS_2 using HfO_2 as a gate insulator has been experimentally implemented [21]. These extraordinary properties have made monolayer MoS_2 an interesting material in optoelectronic devices and next-generation FET. Also, the transition from indirect to direct bandgap upon thinning shows excellent photoluminescence in 2D monolayer [24]. Albeit various brilliant investigations have been performed on the basic and electronic properties of MoS_2 [25-28]. The size-subordinate tunability of the electronic properties makes MoS_2 a novel material for nanoscale field-effect transistors and optical sensors [29-31]. However, as far as we could possibly know, the impact of SOC on both bulk and monolayer MoS_2 band structure has not been widely examined.

In this study, the band structure of bulk and monolayer MoS_2 were numerically investigated by the plane-wave based CASTEP, and local density approximation (LDA) and generalized gradient approximation (GGA) exchange-correlation functional were used. The influence of the spin-orbit coupling (SOC) effect on the electronic energy band structure of both monolayer and bulk MoS_2 has also been calculated in this study. Our results indicate that both bulk and monolayer MoS_2 materials are very good candidates for Opto- and spintronic device applications.

COMPUTATIONAL METHOD

First principle's calculation based on the pseudopotential plane-wave method [32] is executed in the Cambridge serial total energy package (CASTEP) [33]. This method has been used to study the electronic properties of monolayer GeI [34] and bulk and monolayer WSe_2. The generalized gradient approximations (GGA) of Perdew-Burke-Ernzerhof (PBE) and Local density approximations (LDA) functional [35, 36] including the spin-orbit coupling (SOC) [37] for exchange-correlation interactions. Furthermore, norm-conserving pseudopotential was used in the treatment of ion-electron exchange. The energy cut off for all calculations in this work was 700 eV, for both bulk and monolayer MoS_2, a k-points separation of 0.015/angstrom and SCF tolerance of 1.0×10^{-6} eV/atom were employed. The electronic minimizer was set to all bands/EDFT. Generally, the density mixing is the proposed choice for electronic minimizer, but to perform the calculation with SOC effect, the required electronic minimizer is set to all bands/EDFT in order to make a meaningful

comparism. The Monkhorst-Pack K-point was set to $7\times7\times7$ and $7\times7\times1$ for bulk and monolayer respectively. For monolayer MoS_2 case, we created 20 Å vacuum along Z axis in order to prevent any interaction between the layers. The pseudo atomic calculation performed for S: $3S^2, 3P^4$ and Mo: $4d^5, 5S^1$. The simulation of the band structure is performed in high symmetry direction $\Gamma - M - K - \Gamma$.

RESULTS

Structural parameters

Molybdenum disulfide has a hexagonal crystal structure linked to space group P 6_3/mmc (194). The structure is made up of the stacking of three atomic layers S-Mo-S layer. Monolayer MoS_2 has a single S-Mo-S layer as shown in Fig. 1b, whiles the bulk MoS_2 has a two-layer monolayer MoS_2 with one-layer Mo atoms place on top of the Sulphur atoms of the other layer, illustrated in Fig. 1b. From geometry optimization, the lattice constants for bulk MoS_2 are 3.192A in a and b axis and 12.478 in the c-axis. The monolayer slab was cleaved in 001 direction and a vacuum layer of 20A.

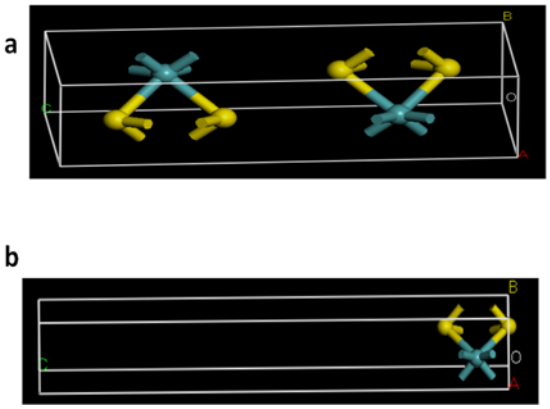

Figure 1. A ball and stick model of one-unit cell of the (a) bulk MoS_2 and (b) Monolayer MoS_2. The blue atoms represent the Mo atoms, and the yellow atoms represent the S atoms.

Electronic properties and density of states

A series of calculations were performed on the bulk and monolayer MoS_2 with LDA CAPZ and GGA PBE functionals incorporated with or without SOC. The electronic band pattern of monolayer MoS_2 as shown in Fig. 2 has a direct bandgap situated at $K \to K$ of k point.

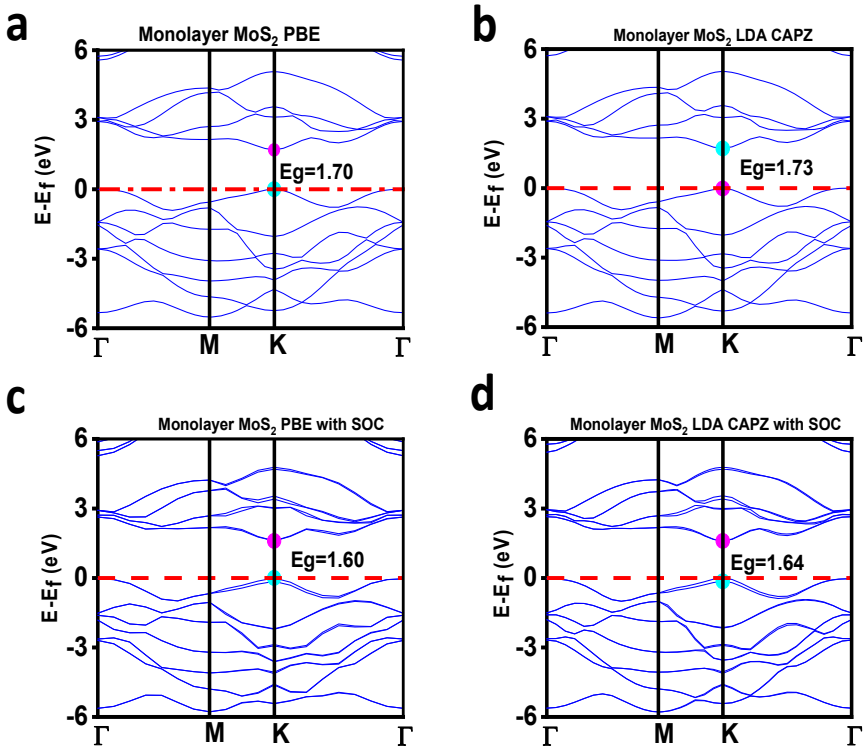

Figure 2. Band structure of (a)-monolayer MoS_2 PBE without SOC, (b)-Monolayer LDA CAPZ without SOC, (c)-Monolayer MoS_2 PBE with SOC, (d)-Monolayer MoS_2 LDA CAPZ with SOC

This transition in bandgap makes monolayer MoS_2 applicable to different devices. Interestingly, all the calculations either with or without SOC captures the direct bandgap feature for monolayer MoS_2. Also, the application of SOC for monolayer MoS_2 affects the band gap value. Furthermore, the valence band maximum and that of the conduction band both occur at high symmetric K point indicating a direct bandgap semiconductor as shown in Fig. 2(a-d) above. The bandgap value for monolayer MoS_2 ranges from 1.60 to 1.71eV. The experimental result indicates a slight shift from the theoretical result. The theoretical work gives a slight difference in bandgap than the experiment as illustrated in Table.

Table

Energy band gap (eV) and bandgap type for both Bulk and Monolayer

	Bulk MoS_2		Monolayer MoS_2	
Functionals	Indirect bandgap	Bandgap value	Direct bandgap	Bandgap value
GGA PBE no SOC	Yes	1.27	Yes	1.70
LDA CAPZ no SOC	Yes	1.23	Yes	1.73
GGA PBE SOC	Yes	1.22	Yes	1.60
LDA CAPZ SOC	Yes	1.17	Yes	1.64
EXP REF	Yes	1.23(ref [19]) 1.29(ref [27])	Yes	1.80 (ref [19])
THEOR REF	Yes	0.7(ref [38]) 1.05(ref [26]) 1.15(ref [39])	Yes	1.55 (ref [25,26]) 1.70 (ref [40]) 1.78 (ref [41]) 1.9 (ref [42])

From Fig. 2(a-d), the valence band maximum (VBM) and the conduction band minimum (CBM) lie below and above the Femi level respectively along with the K- symmetry. For the monolayer MoS_2, there is a reasonable band splitting as seen in Fig 2 (c) and (d), this band splitting is brought about by the utilization of SOC and can likewise help in the application of spintronic and valleytronics [43-47]. The band splitting is observed distinctly in the valence band (VB) of the high symmetry K-direction. This result is good agreement with previously reported literature [28, 43, 48].

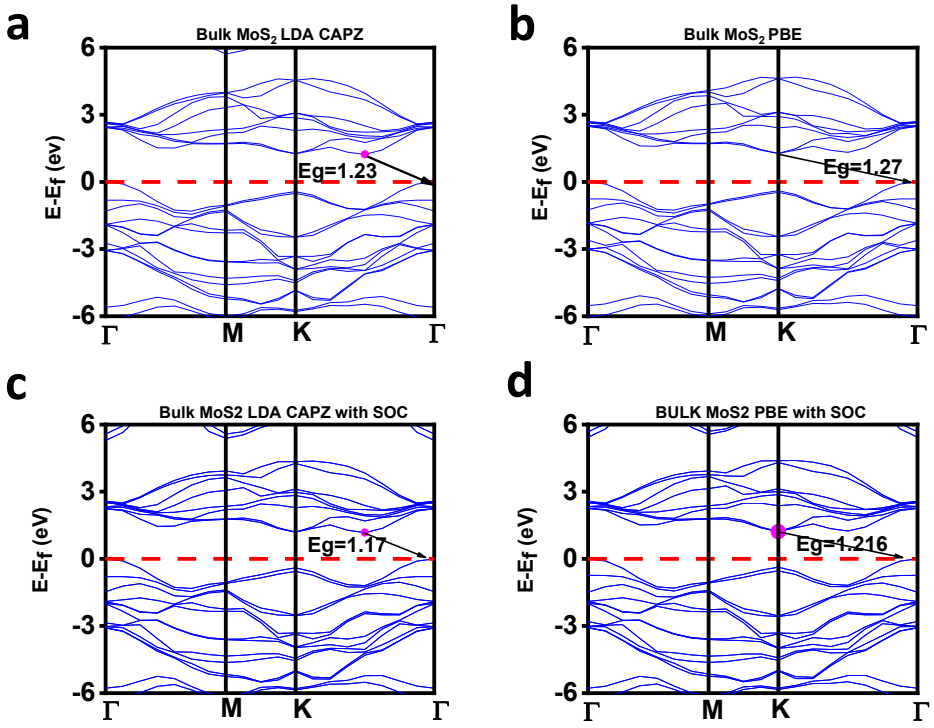

Figure 3. Band structure of (a) Bulk MoS_2 PBE without SOC (b) Bulk LDA CAPZ without SOC (c) Bulk MoS_2 PBE with SOC (d) Bulk MoS_2 LDA CAPZ with SOC

Fig. 3. (a)- (d) represents the band structure of bulk MoS_2 for PBE and LDA functionals. The band structure profiles obtained indicate an indirect semiconductor since the maxima of the valence band is situated at K Γ - path whiles that of the minimum of the conduction band is located at Γ -point. The obtained bandgap values range from 1.17-1.27 eV which is consistent with the experimental value [19, 27] shown in Table. From the obtained results of the electronic structures,

we realized that there are slight changes in the energy band with or without SOC. Also, it was observed that the bandgap value 0f the compound with SOC is smaller than the one without SOC. Fig. 3 (c) and (d) show a slight Valence band (VB) splitting on a high symmetry K direction. This splitting can be ascribed to the utilization of SOC [43, 49-53]. The SOC influences the valence band of the compound as appeared in Fig. 3(c,d).

Fig. 4. (a-d) represents the partial density of states of bulk and monolayer MoS_2 using two different functionals i.e. PBE and LDA. MoS_2 exhibits a neutral charge due to the presence of +4 in the valence of Mo and a charge of -2 for the S- atom. From Fig. 4(a-d), the partial density of states can be divided into three classes of states. For the first class, the density around -14eV is due to 3s orbital of S atom which is separated by a wide gap. The second class is the one below the Fermi level in which the contributing orbitals the 3p orbitals of S atom and 4d orbitals of Mo. This class possesses a strong hybridization. The third class is the one above the Fermi-level, here the contributing orbital is the 4d orbitals of Mo and is separated by the second class with a narrow gap. For both functionals, the bandgap occurs due to the 4d orbitals of Mo and 3p orbitals of S atoms in monolayer and bulk MoS_2.

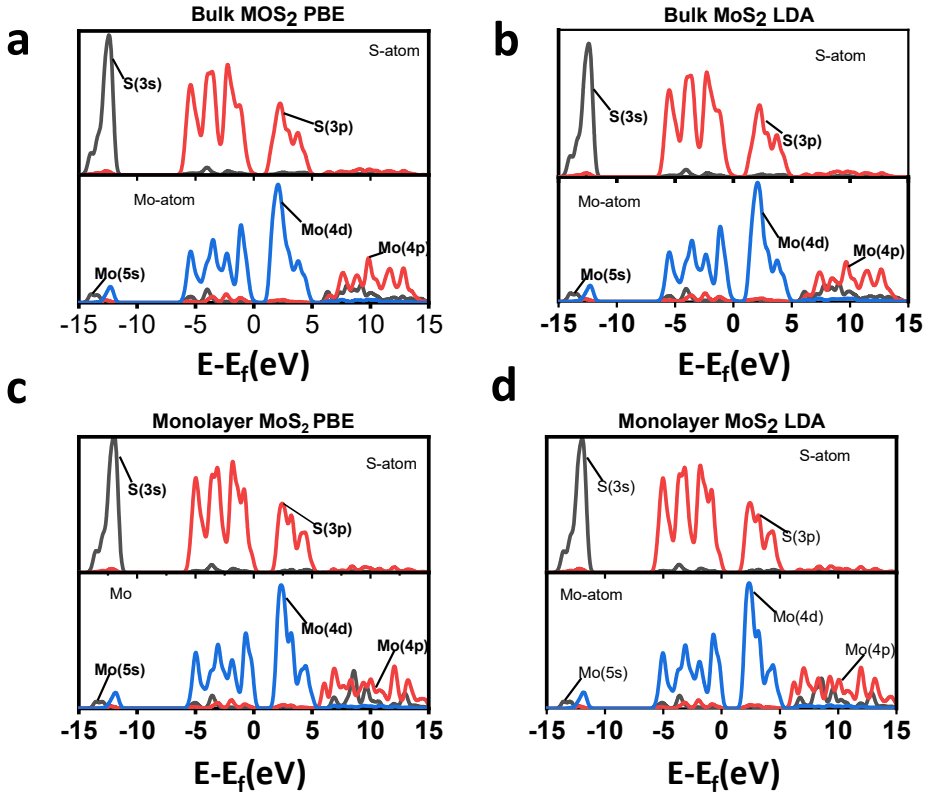

Figure 4. Partial density of states of (a) Bulk MoS_2 using PBE functional (b) Bulk MoS_2 using LDA (c) MoS_2 monolayer using PBE functional (d) MoS_2 monolayer using LDA

CONCLUSION

The electronic properties of bulk and monolayer MoS_2 have been studied using first-principle calculations based on the pseudopotential plane-wave method. Our results show that monolayer MoS_2 is a direct semiconductor whiles bulk MoS_2 has an indirect bandgap. Also, our calculations show that the bandgap of monolayer MoS_2 ranges from 1.6-1.73 eV whereas the bulk is 1.17-1.27 eV which is consistent with the available experimental and theoretical results. The electronic structure and density of states indicate many similarities between the monolayer and bulk MoS_2. The main contribution to the valence and conduction band are 4d states of Mo and 3p orbitals of s atom in both monolayer and bulk MoS_2. We have discovered that the incorporation of spin-orbit coupling influences the band structures and the splitting of degenerate valence band occurs on high symmetry K-point.

Conflict of interest

The authors declare that they have no conflict of interest.

Funding

This research did not receive any specific grant from funding agencies in the public, commercial, or not-for-profit sectors.

ORCID IDs

Michael Gyan, https://orcid.org/0000-0001-6337-2205; **Francis E. Botchway**, https://orcid.org/0000-0001-8327-4469;
Joseph Parbey, https://orcid.org/0000-0002-0277-0098

REFERENCES

[1] K.S. Novoselov, D. Jiang, F. Schedin, T.J. Booth, V.V. Khotkevich, S.V. Morozov, and A.K. Geim, PNAS, **102**(30), 10451-10453 (2005), https://doi.org/10.1073/pnas.0502848102.
[2] W. Choi, I. Lahiri, R. Seelaboyina, and Y.S. Kang, Critical Reviews in Solid State and Materials Sciences, **35**, 52-71 (2010), https://doi.org/10.1080/10408430903505036
[3] M.J. Allen, V.C. Tung, and R.B. Kaner, Chemical Reviews, **110**(1), 132-145 (2010), https://doi.org/10.1021/cr900070d.
[4] H. Liu, A.T. Neal, Z. Zhu, Z. Luo, X. Xu, D. Tománek, and P.D. Ye, ACS Nano. **8**(4), 4033-4041 (2014), https://doi.org/10.1021/nn501226z.
[5] B. Lalmi, H. Oughaddou, H. Enriquez, A. Kara, S. Vizzini, B. Ealet, and B. Aufray, Applied Physics Letters, **97**(22), 223109 (2010), https://doi.org/10.1063/1.3524215.
[6] Q.H. Wang, K. Kalantar-Zadeh, A. Kis, J.N. Coleman, and M.S. Strano, Nature Nanotechnology, **7**(11), 699-712 (2012), https://doi.org/10.1038/nnano.2012.193.
[7] M. Safari, Z. Izadi, J. Jalilian, I. Ahmad, and S. Jalali-Asadabadi, Physics Letters A, **381**(6), 663-670 (2017), https://doi.org/10.1016/j.physleta.2016.11.040.
[8] S. Das, J.A. Robinson, M. Dubey, H. Terrones, and M. Terrones, Annual Review of Materials Research, **45**(1), 1-27 (2015), https://doi.org/10.1146/annurev-matsci-070214-021034.
[9] D.J. Late, B. Liu, H. Matte, C.N.R. Rao, and V.P. Dravid, Advanced Functional Materials, **22**(9), 1894-1905 (2012), https://doi.org/10.1002/adfm.201102913.
[10] C.V. Nguyen, N.N. Hieu, D. Muoi, C.A. Duque, E. Feddi, H.V. Nguyen, L.T.T. Phuong, B.D. Hoi, and H.V. Phuc, Journal of Applied Physics, 123(3), 034301 (2018), https://doi.org/10.1063/1.5009481.
[11] M.H. Fekri, R. Bazvand, M. Soleymani, and M.R. Mehr, International Journal of Nano Dimension, **11**(4), 346-354 (2020), http://www.ijnd.ir/article_675374_91ad4efdd80a983d0ba8492569c8e510.pdf.
[12] W. Zhang, Z. Huang, W. Zhang, and Y. Li, "Two-Dimensional Semiconductors with Possible High Room Temperature Mobility," Nano Research, **7**(12), 1731-1737 (2014), https://doi.org/10.1007/s12274-014-0532-x.
[13] M. Khaleghian, and F. Azarakhshi, International Journal of Nano Dimension, **10**(1), 105-113 (2019), http://www.ijnd.ir/article_661564_d54fcf021f466ebbe353d21c7a171061.pdf.
[14] J.A. Wilson, and A.D. Yoffe, Advances in Physics, **18**(73), 193-335 (1969), https://doi.org/10.1080/00018736900101307.
[15] Y. Kim, J.L. Huang, and C.M. Lieber, Applied Physics Letters, **59**(26), 3404-3406 (1991), https://doi.org/10.1063/1.105689.
[16] A.H. Reshak, and S. Auluck, Physical Review B, **68**, 125101 (2003), https://doi.org/10.1103/PhysRevB.68.125101.
[17] E. Fortin and W.M. Sears, Journal of Physics and Chemistry of Solids. **43**(9), 881-884 (1982), https://doi.org/10.1016/0022-3697(82)90037-3.
[18] K.H. Hu, X.G. Hu, and X.J. Sun, Applied Surface Science, **256**(8), 2517-2523 (2010), https://doi.org/10.1016/j.apsusc.2009.10.098.
[19] K.F. Mak, C. Lee, J. Hone, J. Shan, and T.F. Heinz, Physical Review Letters, **105**(13), 36805 (2010), https://doi.org/10.1103/PhysRevLett.105.136805.
[20] P. Joensen, R.F. Frindt, and S.R. Morrison, Materials Research Bulletin, **21**(4), 457-461 (1986), https://doi.org/10.1016/0025-5408(86)90011-5.
[21] B. Radisavljevic, A. Radenovic, J. Brivio, V. Giacometti, and A. Kis, Nature Nanotechnology, **6**, 147 (2011), https://doi.org/10.1038/nnano.2010.279.
[22] J.N. Coleman, M. Lotya, A. O'Neill, S.D. Bergin, P.J. King, U. Khan, K. Young, A. Gaucher, S. De, R.J. Smith, I.V. Shvets, S.K. Arora, G. Stanton, H.-Y. Kim, K. Lee, G.T. Kim, G.S. Duesberg, T. Hallam, J.J. Boland, J.J. Wang, J.F. Donegan, J.C. Grunlan, G. Moriarty, A. Shmeliov, R.J. Nicholls, J.M. Perkins, E.M. Grieveson, K. Theuwissen, D.W. McComb, P.D. Nellist, and V. Nicolosi, Science, **331**(6017), 568-571 (2011), https://doi.org/10.1126/science.1194975.
[23] D. Dey, and D. De, Int. J. Nano Dimens. **9**(2), 134-144 (2018), http://www.ijnd.ir/article_658988_772299c871dafd993e3f08bec602d2a1.pdf.
[24] J.K. Ellis, M.J. Lucero, and G.E. Scuseria, Applied Physics Letters, **99**(26), 261908 (2011), https://doi.org/10.1063/1.3672219.
[25] S. Ahmad, and S. Mukherjee, Graphene, **3**, 52-59 (2014), http://dx.doi.org/10.4236/graphene.2014.34008.
[26] A. Kumar, and P.K. Ahluwalia, Materials Chemistry and Physics, **135**(2), 755-761 (2012), https://doi.org/10.1016/j.matchemphys.2012.05.055.
[27] Th. Böker, R. Severin, A. Müller, C. Janowitz, R. Manzke, D. Voß, P. Krüger, A. Mazur, and J. Pollmann, Physical Review B, **64**, 235305 (2001), https://doi.org/10.1103/PhysRevB.64.235305
[28] D.P. Rai, T.V. Vu, A. Laref, Md.A. Hossain, E. Haque, S. Ahmad, R. Khenatag, and R.K. Thapah, RSC Advances, **10**(32), 18830-18840 (2020), https://doi.org/10.1039/D0RA02585B.
[29] F.J. Urbanos, A. Black, R. Bernardo-Gavito, A.L. Vázquez de Parga, R. Miranda, and D. Granados, Nanoscale, **11**(23), 11152-11158 (2019), https://doi.org/10.1039/c9nr02464f.
[30] Tung Pham, Guanghui Li, Elena Bekyarova, Mikhail E. Itkis, and Ashok Mulchandani, ACS Nano, **13**(3), 3196-3205 (2019), https://doi.org/10.1021/acsnano.8b08778.
[31] N. Goel, R. Kumar, and M. Kumar, *AIP Conference Proceedings*, **1942**(1), 050060 (2018), https://doi.org/10.1063/1.5028691.
[32] M.D. Segall, P.J.D. Lindan, M.J. Probert, C.J. Pickard, P.J. Hasnip, S.J. Clark, and M.C. Payne, Journal of Physics: Condensed Matter, **14**(11), 2717-2744 (2002), https://doi.org/10.1088/0953-8984/14/11/301.
[33] S.J. Clark, M.D. Segall, C.J. Pickard, P.J. Hasnip, M.I.J. Probert, K. Refson, and M.C. Payne, Zeitschrift für Kristallographie. 220(5-6), 567-570 (2005), https://doi.org/10.1524/zkri.220.5.567.65075.
[34] D.M. Hoat, T.V. Vu, M.M. Obeid, and H.R. Jappor, Chemical Physics, **527**, 110499 (2019), https://doi.org/10.1016/j.chemphys.2019.110499.
[35] J.P. Perdew, K. Burke, and M. Ernzerhof, Physical Review Letters, **77**(18), 3865-3868 (1996), https://doi.org/10.1103/PhysRevLett.77.3865.
[36] J.P. Perdew, K. Burke, and M. Ernzerhof, Phys. Rev. Lett. 77, 3865 (1996)]," Physical Review Letters, **78**(7), 1396-1396 (1997), https://doi.org/10.1103/PhysRevLett.77.3865.
[37] A.H. MacDonald, W.E. Picket, and D.D. Koelling, Journal of Physics C: Solid State Physics, **13**(14), 2675-2683 (1980), https://doi.org/10.1088/0022-3719/13/14/009.
[38] K. Kobayashi, and J. Yamauchi, Surface Science, **357-358**, 317-321 (1996), https://doi.org/10.1016/0039-6028(96)00173-2.

[39] L.F. Mattheiss, Physical Review Letters, **30**, 784-787 (1973), https://doi.org/10.1103/PhysRevLett.30.784.
[40] C. Ataca, and S. Ciraci, The Journal of Physical Chemistry C, **115**(27), 13303-13311 (2011), https://doi.org/10.1021/jp2000442.
[41] S. Lebègue, and O. Eriksson, Physical Review B, **79**(11), 115409 (2009), https://doi.org/10.1103/PhysRevB.79.115409.
[42] A. Kuc, N. Zibouche, and T. Heine, Physical Review B, **83**(24), 245213 (2011), https://doi.org/10.1103/PhysRevB.83.245213.
[43] Z.Y. Zhu, Y.C. Cheng, and U. Schwingenschlögl, Physical Review B, **84**(15), 153402 (2011), https://doi.org/10.1103/PhysRevB.84.153402.
[44] D. Xiao, G.-B. Liu, W. Feng, X. Xu, and W. Yao, Physical Review Letters, **108**(19), 196802 (2012), https://doi.org/10.1103/PhysRevLett.108.196802.
[45] H. Zeng, J. Dai, W. Yao, D. Xiao, and X. Cui, Nature Nanotechnology, **7**(8), 490-493 (2012), https://doi.org/10.1038/nnano.2012.95.
[46] M. Bieniek, L. Szulakowska, and P. Hawrylak, Physical Review B, **101**(3), 035401 (2020), https://doi.org/10.1103/PhysRevB.101.035401.
[47] Q. Chen, L. Liang, G. Potsi, P. Wan, J. Lu, T. Giousis, E. Thomou, D. Gournis, P. Rudolf, and J. Ye, Nano Letters, **19**(3), 1520-1526 (2019), https://doi.org/10.1021/acs.nanolett.8b04207.
[48] C.-H. Chang, X. Fan, S.-H. Lin, and J.-L. Kuo, Physical Review B, **88**(19), 195420 (2013), https://doi.org/10.1103/PhysRevB.88.195420.
[49] D.Y. Qiu, F.H. da Jornada, and S.G. Louie, Physical Review Letters, **111**(21), 216805 (2013), https://doi.org/10.1103/PhysRevLett.111.216805.
[50] A. Molina-Sánchez, D. Sangalli, K. Hummer, A. Marini, and L. Wirtz, Physical Review B, **88**(4), 045412 (2013), https://doi.org/10.1103/PhysRevB.88.045412.
[51] N. Alidoust, G. Bian, S.-Y. Xu, R. Sankar, M. Neupane, C. Liu, I. Belopolski, D.-X. Qu, J.D. Denlinger, F.-C. Chou, and M.Z. Hasan, Nature Communications, **5**, 4673 (2014), https://doi.org/10.1038/ncomms5673.
[52] X. Dou, K. Ding, D. Jiang, X. Fan, and B. Sun, ACS Nano. **10**(1), 1619-1624 (2016), https://doi.org/10.1021/acsnano.5b07273.
[53] N. Zibouche, A. Kuc, J. Musfeldt, and T. Heine, Annalen der Physik, **526**(9-10), 395-401 (2014), https://doi.org/10.1002/andp.201400137.

ПОЧАТКОВІ ДОСЛІДЖЕННЯ ЕЛЕКТРОННИХ ВЛАСТИВОСТЕЙ ОБ'ЄМНОГО ТА ОДНОШАРОВОГО MoS_2 З ВИКОРИСТАННЯМ ДПФ: ЗАСТОСУВАННЯ ПАРАМЕТРІВ СПІН-ОРБІТАЛЬНОГО ЗВ'ЯЗКУ (SOC)

Майкл Гайян[a], Френсіс Е. Ботвей[b,c], Джозеф Парбі[a,b,c]
[a]Китайська школа фізики Університету електронних наук і технологій Китаю, Ченду 610054, Китай
[b]Школа матеріалознавства, Китайський університет електронних наук і технологій, Ченду, 610054, Китай
[c]Кофорідва, Технічний університет, Гана

Двомірні (2D) матеріали в даний час викликають великий інтерес завдяки чудовим властивостям, що відрізняють їх від об'ємних структур. Одношарові та багатошарові дихалькогеніди перехідних металів (TMDC) мають ширину забороненої зони, яка коливається в межах 1-2 еВ, що використовується для пристроїв FET або будь-яких оптоелектронних пристроїв. У випадку TMDC розгляд зосереджено на дисульфіді молібдену (MoS_2) через перспективи регулювання забороненої зони, а перехід між властивостями прямих та непрямих переходів зони залежить від його товщини. Розрахунки теорії щільності функціонала (DFT) з різними функціоналами та параметрами спін-орбітальної зв'язку (SOC) проводились для вивчення електронних властивостей об'ємного та одношарового MoS_2. Додавання SOC спричинило помітну зміну профілю енергії зони, явно розділивши максимум валентної зони (VBM) на два діапазони. Зона з непрямими переходами об'ємного MoS_2 коливається в межах 1,17-1,71 еВ, а зона у випадку одного шару становить 1,6-1,71 еВ. Розраховані параметри порівнювали з отриманими експериментальними та теоретичними результатами. Отримана щільність станів (DOS) може бути використана для пояснення природи зони як в об'ємному, так і в одношаровому MoS_2. Ці електронні характеристики важливі для застосування в матеріальних пристроях та енергозберігаючих застосуваннях.

КЛЮЧОВІ СЛОВА: електронні властивості, теорія щільності функціонала, спін-орбітальний зв'язок, щільність станів, MoS_2, заборонена зона

ПЕРВОНАЧАЛЬНЫЕ ИССЛЕДОВАНИЯ ЭЛЕКТРОННЫХ СВОЙСТВ ОБЪЕМНОГО И ОДНОСЛОЙНОГО MoS_2 С ИСПОЛЬЗОВАНИЕМ ДПФ: ПРИМЕНЕНИЕ ПАРАМЕТРОВ СПИН-ОРБИТАЛЬНОЙ СВЯЗИ (SOC)

Майкл Гайян[a], Фрэнсис Э. Ботвей[b,c], Джозеф Парби[a,b,c]
[a]Китайська школа физики Университета электронных наук и технологий Китая, Чэнду 610054, Китай
[b]Школа материаловедения, Китайский университет электронных наук и технологий, Чэнду, 610054, Китай
[c]Кофоридва, Технический университет, Гана

Двухмерные (2D) материалы в настоящее время вызывают большой интерес благодаря замечательным свойствам, отличающих их от объемных структур. Однослойные и многослойные дихалькогениды переходных металлов (TMDC) имеют ширину запрещенной зоны, которая колеблется в пределах 1-2 эВ, что используется для устройств FET или любых оптоэлектронных устройств. В случае TMDC рассмотрение сосредоточено на дисульфиде молибдена (MoS_2) из-за перспективы регулирования запрещенной зоны, а переход между свойствами прямых и косвенных переходов зоны зависит от его толщины. Расчеты теории плотности функционала (DFT) с различным функционалом и параметрами спин-орбитальной связи (SOC) проводились для изучения электронных свойств объемного и однослойного MoS_2. Добавление SOC привело к заметному изменению профиля энергии зоны, явно разделив максимум валентной зоны (VBM) на два диапазона. Зона с косвенным переходами объемного MoS_2 колеблется в пределах 1,17-1,71 эВ, а зона в случае одного слоя составляет 1,6-1,71 эВ. Рассчитаные параметры сравнивали с полученными экспериментальными и теоретическими результатами. Полученная плотность состояний (DOS) может быть использована для объяснения природы зоны как в объемном, так и в однослойном MoS_2. Эти электронные характеристики важны для применения в материальных устройствах и энергосберегающих приложениях.

КЛЮЧЕВЫЕ СЛОВА: электронные свойства, теория плотности функционала, спин-орбитальная связь, плотность состояний, MoS_2, запрещенная зона